Electron acceleration from underdense plasma with the Vulcan Petawatt laser

S. R. Nagel, S. P. D. Mangles, S. Kneip, C. Bellei, L. Willingale, A. E. Dangor and Z. Najmudin
The Blackett Laboratory, Imperial College London, Prince Consort Road, London, SW7 2BW, UK

R. J. Clarke, R. Heathcote and K. L. Lancaster
Central Laser Facility, STFC, Rutherford Appleton Laboratory, Chilton, Didcot, Oxon, OX11 0QX, UK

A. Gopal and M. Tatarakis
Technological Educational Institute of Crete, Chania, Crete, Greece

A. Maksimchuk, S. A. Reed and K. Krushelnick
University of Michigan, 1006 Gerstacker, Ann Arbor, MI 48109, USA

Main contact email address **s.nagel@imperial.ac.uk**

Introduction

The advance in laser technology to ultra-high intense ($\geq 10^{18}$Wcm^{-2}) short-pulse ($\leq$1ps) lasers has made it possible to study laser-plasma interactions at ultra-high intensities. Applications include particle accelerators [1], inertial confinement fusion schemes [2] and also biological and medical technologies. In conventional particle accelerators, the electric field used to accelerate charged particles is limited by electrical breakdown, to a maximum of the order of 50MVm^{-1} [3]. Plasmas are already ionised so are unaffected by the problems associated with material breakdown at high field strength. The use of laser excited plasma oscillations to accelerate electrons was first proposed by Tajima and Dawson [1].

Experimental data on electron acceleration obtained with the Vulcan petawatt laser is presented. With the "long" pulse length that Vulcan features ($\geq$500fs) electron densities of $\leq 10^{16}$cm^{-3} would be necessary, in order to satisfy the optimal condition for laser wakefield acceleration (LWFA) which requires that the laser pulse length = half the plasma wavelength. At these densities the dephasing length would be on the order of tens of meters. With the laser parameters in the discussed experiment, namely intensities $\geq 10^{20}$Wcm^{-2} ($a_0 >> 1$) and laser pulse lengths of approximately 700fs, at densities between 10^{18}cm^{-3} to 10^{20}cm^{-3}, the dominant acceleration mechanism is direct laser acceleration (DLA) [4,5]. DLA usually relies on another electron acceleration mechanism, i.e. SMLWFA, to initially accelerate the electrons until they reach an energy (γ_e) at which the resonance condition for the betatron resonance mechanism is satisfied. The resonance condition occurs when the laser frequency as witnessed by an electron, moving in the laser direction, is the same as the oscillation or bounce frequency of the channel. This resonance condition can be expressed in terms of background plasma density and laser intensity:

$$\gamma_e \approx 4\frac{n_c^2}{n_e^2}\left(1+\frac{a_0^2}{4}\right)^2 \nabla \mathbf{F}$$

where **F** is the focusing force due to the combination of magnetic and electric fields. In the blow out regime and the case of constant intensity $\gamma_e \propto (1/n_e)$ [6].

It has been found previously [7] that self-guiding of the laser pulse is favoured for bigger focal spots.

In this report we are looking at how different f-numbers influence the acceleration of electrons with comparable laser energy and pulse length. The change in focal spot size, due to the difference in focusing, leads to a difference in intensity and Rayleigh length. Optimal densities for electron acceleration are observed, as well as a shift of this density with f-number.

Experimental setup

The experiment described was performed using the Vulcan Petawatt Laser. The laser was focused with either f/3 or f/5 focusing geometry; the energy on target was kept constant at 85J. For the two different f-numbers, f/3 and f/5, the laser had a duration of (630±120)fs and (760±100)fs respectively. This change in pulse length was due to a loss of bandwidth for the apodised (f/5) beam. The operation wavelength of Vulcan is 1055nm. For this wavelength the non-relativistic critical density is $n_c = 1\times10^{21}$cm^{-3}. A focal spot measurement, for the case of f/3, at low power gave a FWHM of approximately 5μm. From this we can infer a FWHM of about 9μm for the case of f/5. Therefore the intensities for f/3 and f/5 can be estimated to be 2.5×10^{21}Wcm^{-2} and 1.1×10^{20}Wcm^{-2} respectively. The spot size also influences the Rayleigh length ($z_R \approx 2 \bullet f_{\#} \bullet FWHM$), which then becomes approximately 30μm for the case of f/3 and 90μm for the case of f/5.

The supersonic gas jet nozzle creates a gas column with a sharp interface between the gas and the surrounding vacuum. By focusing the laser into the gas, underdense plasma is formed. The plasma density can be controlled by varying the backing pressure of the gas reservoir. Helium is used as a target material. The electron plasma frequency can be found by the forward Raman scattered laser spectra. From the plasma frequency, the electron density n_e can be obtained, since $\omega_p = \sqrt{n_e e^2/(m_e \varepsilon_0)}$, where e is the electron charge, m_e is the electron mass. The density shows a linear dependence on the backing pressure.

The electrons were measured in the direction of the laser propagation at 0°. A 7.3mm slit was placed in front of the entrance to the electron spectrometer, to limit the angular acceptance and hence improve the energy resolution. The slit size was chosen as a compromise between the energy resolution of the electrons and signal level and size for the detection of x-rays emitted from the interaction (see [8]). The accelerated electrons pass through a magnetic field. The Lorentz force deflects the electrons away from their axis

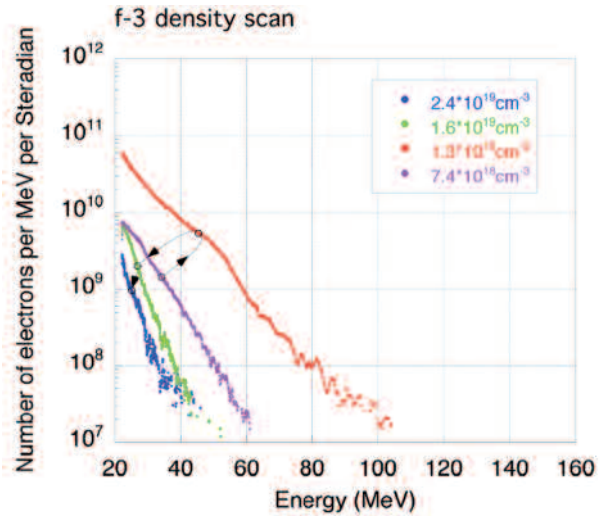

Figure 1. Electron spectra for density scan with f/3.

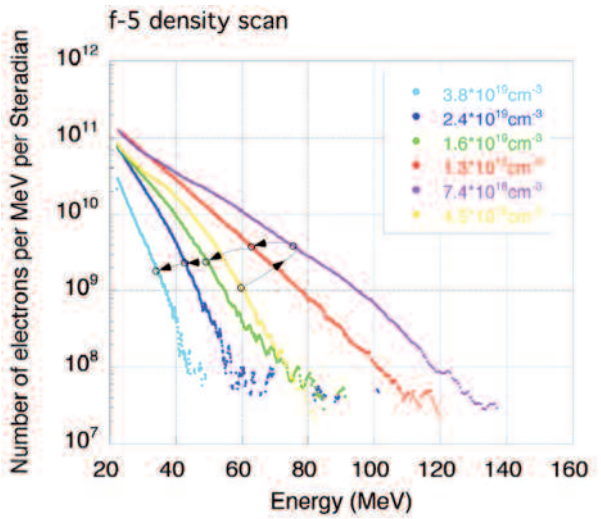

Figure 2. Electron spectra for density scan with f/5.

of propagation. In this experiment the electron spectrometer was run with a field strength of 0.2T. In addition to the electron spectrometer, electron beam divergence stacks were used to discern the electron beam divergence above a certain energy threshold. A stack is made of layers of metal and detectors. Depending on the detectors position in the stack it detects electrons above a certain energy threshold. The stack was placed 10 cm behind laser focus.

Results

Figure 1 and 2 show electron spectra for density scans taken with f/3 and f/5 respectively. In the electron spectra the number of electrons per MeV per steradian (log scale) is plotted versus the energy of the electrons. The different colours correspond to different electron densities. The effective temperatures of the electrons can be obtained by exponential fits to the spectra ($y = A \bullet \exp(E^{MeV}/T_{eff}^{MeV})$).

The so obtained values for the effective temperature as well as the observed maximum energies are plotted against electron density in figure 3. The maximum energy and effective temperature are about a factor of ten different, but follow the same trend with density. One can easily see that both density scans show an optimum density (large T_{eff} and E_{max}). This variation of energy with density has been observed before[4]. At first the total charge and effective temperature increase with decreasing density. This is in agreement with the scaling of the electron energy at which betatron resonance occurs $\gamma_e \propto (1/n_e)$, see figure 4. At densities below the optimum the initial trapping and LWFA of the electrons is unlikely and hence less electrons will be injected into the channel. This density scaling can be found for both f-numbers. An intensity scan taken on this experimental run, using f/3 focusing, shows that LWFA is more likely to occur for lower a_0. As the intensity decreases, the shape of the electron spectra becomes less maxwellian, indicating that LWFA is the dominant acceleration mechanism. The effective temperatures for the higher a_0 also scale with γ_e, indicating DLA to be the dominant acceleration mechanism.

If one only takes the intensity dependence for DLA into account, this would suggest that f/3 focusing, giving a higher a_0 should lead to better electron acceleration than the case of f/5 focusing. However, in the case of f/3 we observe lower temperatures, maximum energies and charge, than in the case of f/5. The acceleration of the electrons is more efficient in the case of f/5 for all observed densities. The f/5 focusing geometry features a larger focal spot, longer pulse length but lower a_0. Since γ_e is also

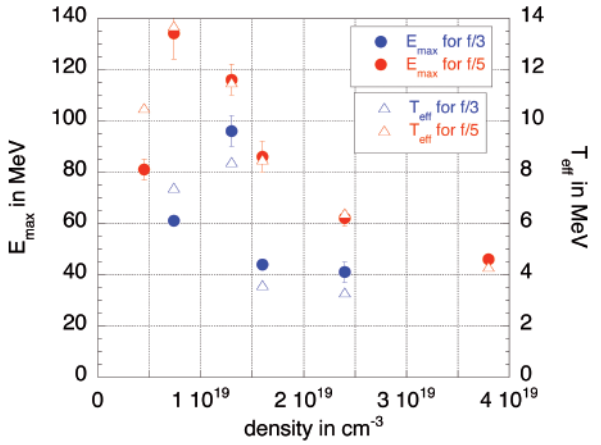

Figure 3. f/3(blue) and f/5(red) comparison for maximum electron energies (dots) and effective temperatures (triangles).

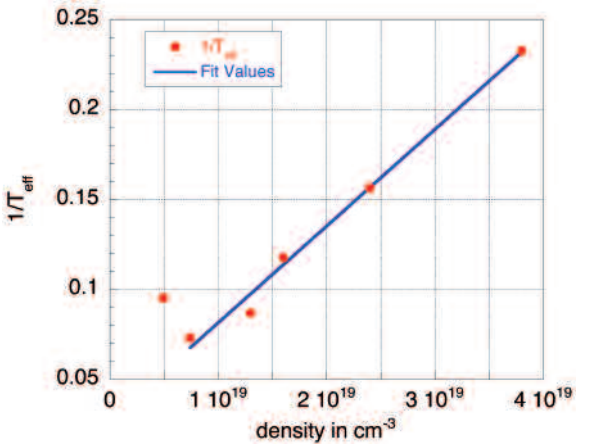

Figure 4. $1/T_{eff}$ for f/5 focusing plotted against density. The blue curve is a linear fit to the data points excluding the one at 4.4×10^{18}cm^{-3}.

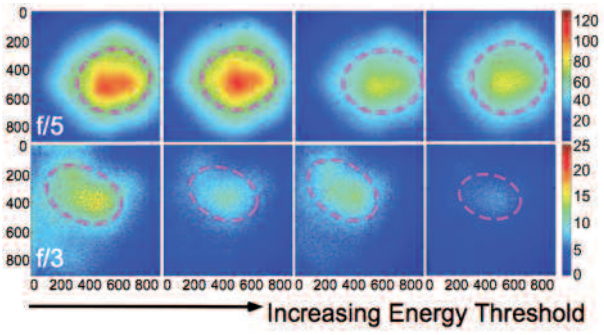

Figure 5. Stack data for the f/5 stack (top), f/3 stack (bottom), energy threshold increases from left to right. The colour bar indicates the number of electrons per pixel. The contours (dashed pink) show the FWHM of the electron beams.

dependent on a_0, $\gamma_e \propto (1+a_0^2/4)^2$, for f/3 γ_e is about a factor of 10 larger than for f/5. Another bonus for the case of f/5 is the longer Rayleigh length which further favours the initial pre-acceleration in the LWFA regime seeding the DLA process with faster electrons. The enlarged focal spot will lead to an increase in channel size, which could support more oscillating electrons in case of f/5 explaining the increase of the accelerated charge from f/3 to f/5. Relativistic self-focusing, which leads to longer propagation length than the Rayleigh length is also dependent on the focal spot size [7]. A bigger spot leading to better self-guiding, increasing the interaction length.

Figure 5 shows the stack data as a number of electrons per pixel. The top row is the image plate detector data for the f/5 shot, and the bottom row for the f/3. The shots were taken at an electron density of 1.3×10^{19}cm^{-3}. As we go through the stack, the signal in case of f/3 drops significantly with increasing energy (low temperatures) whereas in the case of f/5 the signal drops slower (higher temperature). The stack data and the data from the spectrometer show the same trends, namely higher number of electrons are detected in the case of f/5, and the temperature in the case of f/5 is higher as well. The energy to which we observe electrons is higher for the case of f/5.

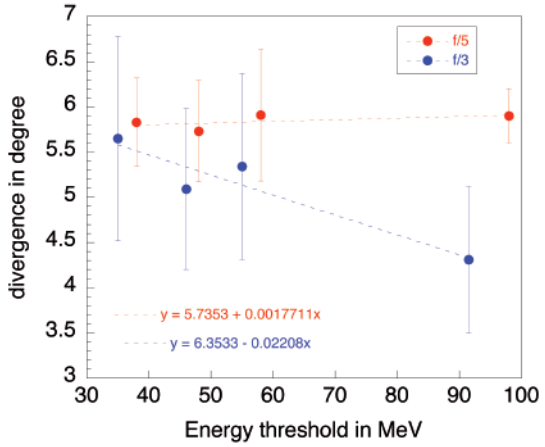

Figure 6. Beam half-angle divergence at the FWHM from the stack data at the different energy thresholds, f/5(blue) and f/3(red) (Half angle). The dotted lines are linear fits to the points.

Figure 6 shows the angle of deflection off the beam axis, for the FWHM (pink contours in figure 5) of the detected electron beam from the stack data. This is plotted against the energy threshold of the detectors position. It can be observed that in the "front" of the stack, the beam divergence is similar for f/3 and f/5. As we go further back in the stack, the divergence for f/5 stays the same, whereas the divergence for f/3 decreases gently. This suggests that in the case of f/5 focusing the electrons pick up radial as well as longitudinal momentum, supporting the assumption that higher energies are accelerated by DLA. For the case of f/3 focusing the acceleration seem to be dominant in the longitudinal direction and less radial, typical of wakefield acceleration [9].

Conclusions

We observe a density dependence for the efficiency of the electron acceleration. This scales like the resonance energy for the betatron resonance acceleration mechanism. For densities below the optimum one, the resonance cannot be reached and LWFA is the dominant acceleration mechanism. For a modest change in f-number (f/5 is only 1.7 times larger than f/3) we observe a significant improvement of the electron acceleration, in electron number and maximum energy, in the case of f/5.

Acknowledgements

The authors acknowledge the assistance of the Central Laser Facility staff at the Rutherford Appleton Laboratory in carrying out this work. This work was supported by the UK Engineering and Physical Science Research Council (EPSRC).

References

1. T. Tajima and J. M. Dawson, *Phys. Rev. Lett.* **43**, 267 (1979).
2. M. Tabak *et al.*, *Phys. Plasmas* **1**, 1626 (1994).
3. E Esarey *et al.*, *IEEE Trans. Plas. Sci.* **24**, 252 (1996).
4. S. P. D. Mangles *et al.*, *Phys. Rev. Lett*. **94**, 245001 (2005).
5. A. Pukhov and J. Meyer-ter Vehn, *Physics of Plasmas* **5**, 1880 (1998);
6. A. Pukhov *et al.*, *Physics of Plasmas* **6**, 2847 (1999).
7. A. G. R. Thomas *et al.*, *Phys. Rev. Lett*. **98**, 095004 (2007).
8. S. Kneip *et al.*, RAL CLF Annual Report 2006/2007.
9. S. P. D. Mangles *et al.*, *Phys. Rev. Lett*. **96**, 215001 (2006).